The 2003 Bam (Iran) earthquake: Rupture of a blind strike-slip fault

Morteza Talebian,[1] Eric J. Fielding,[2,3] Gareth J. Funning,[4] Manoucher Ghorashi,[1]
James Jackson,[5] Hamid Nazari,[1] Barry Parsons,[4] Keith Priestley,[5] Paul A. Rosen,[2]
Richard Walker,[5] and Tim J. Wright[4]

[1] An M_w 6.5 earthquake devastated the town of Bam in southeast Iran on 26 December 2003. Surface displacements and decorrelation effects, mapped using Envisat radar data, reveal that over 2 m of slip occurred at depth on a fault that had not previously been identified. It is common for earthquakes to occur on blind faults which, despite their name, usually produce long-term surface effects by which their existence may be recognised. However, in this case there is a complete absence of morphological features associated with the seismogenic fault that destroyed Bam. *INDEX TERMS:* 1208 Geodesy and Gravity: Crustal movements—intraplate (8110); 1242 Geodesy and Gravity: Seismic deformations (7205); 1243 Geodesy and Gravity: Space geodetic surveys; 6969 Radio Science: Remote sensing. **Citation:** Talebian, M., et al. (2004), The 2003 Bam (Iran) earthquake: Rupture of a blind strike-slip fault, *Geophys. Res. Lett.*, *31*, L11611, doi:10.1029/2004GL020058.

1. Introduction

[2] Bam lies within the western of two north-south, strike-slip fault systems located on each side of the aseismic Lut desert (Figure 1), which together accommodate the relative motion between central Iran and Afghanistan, part of the Eurasian plate [*Jackson and McKenzie*, 1988]. The town lies to the east of the Gowk fault on which several large earthquakes have occurred over the past 23 years [*Berberian et al.*, 1984; *Berberian and Qorashi*, 1994; *Berberian et al.*, 2001]. However, there are no recorded historical earthquakes at Bam, which was for about five hundred years on a flourishing trade route linking Persia with Sistan and Baluchistan [*Ambraseys and Melville*, 1982; *Berberian and Yeats*, 1999]. Most of the citadel, which was destroyed in the earthquake, dated from the Safavid period (1491–1722) [*Matheson*, 1976].

[3] In the immediate aftermath of the earthquake, attention focused on faults whose surface traces, running north-south between Bam and Baravat, are clearly visible on satellite imagery (Figure 1). Field surveys that we carried out in the week after the earthquake found no major surface rupture but showed small-scale fissuring along the fault trace south of the Posht-rud river, and along a 5 km lineament north of the river (Figures 2a and 2b). The northern fault cuts across a featureless plain and is consistent with pure strike-slip faulting. The southern fault appears consistent with a north-south striking, westward-dipping blind thrust fault [e.g., *Lettis et al.*, 1997].

[4] These observations suggested that rupture had occurred at depth on the faults associated with the surface traces. However, in the following section we show an interferogram derived from the first coseismic pair of images obtained by the Advanced Synthetic Aperture Radar (ASAR) on the ESA Envisat spacecraft to become available after the earthquake. The surprising result is that the main
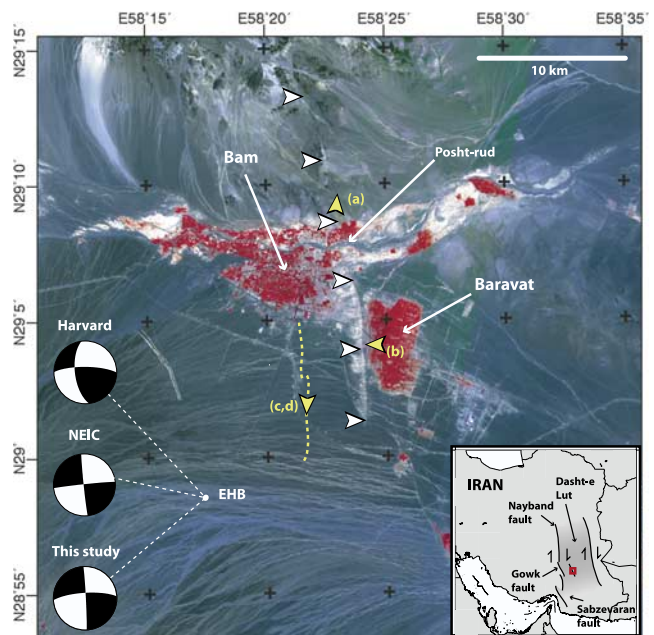

Figure 1. ASTER false colour image of the epicentral region. Red colours indicate the presence of vegetation in the cities of Bam and Baravat (labelled). Focal mechanisms from Harvard, NEIC and this study are shown; the EHB epicentre is provided by E. R. Engdahl (unpublished data, 2004). [White arrowheads: locations of the previously-identified Bam Fault; yellow arrowheads: locations and viewing direction of field photographs in Figure 2; yellow dashed line: surface trace of the newly-revealed blind strike-slip fault responsible for this earthquake.] Inset: location of this area within Iran (red box), with locations of the Nayband-Gowk-Sabzevaran fault system and Dasht-e Lut (Lut desert).

---

[1]Geological Survey of Iran, Tehran, Iran.

[2]Jet Propulsion Laboratory, California Institute of Technology, Pasadena, California, USA.

[3]Also at Centre for the Observation and Modelling of Earthquakes and Tectonics, Department of Earth Sciences, University of Cambridge, Cambridge, UK.

[4]Centre for the Observation and Modelling of Earthquakes and Tectonics, Department of Earth Sciences, University of Oxford, Oxford, UK.

[5]Centre for the Observation and Modelling of Earthquakes and Tectonics, Department of Earth Sciences, University of Cambridge, Cambridge, UK.

Figure 2. Field observations of surface faulting features. Locations and orientations of the photographs are given in Figure 1. (a) Surface rupture north of Bam with en-echelon pattern; (b) Cracking at the foot of the ridge visible in the ASTER image west of Baravat; (c) View southward over en-echelon patterns of surface rupture on the main seismogenic fault south of Bam; (d) Close-up at the locality shown in (c), with right lateral displacement of ~20 cm.

rupture in the earthquake did not occur on faults beneath the obvious surface traces, but on a fault further west, in a region where there is a complete absence of surface features (Figure 1). This fault lies immediately south of Bam and extends directly beneath the city at its northern end.

2. Interferometric Observations of the Bam Earthquake

[5] Since the launch of ERS-1 in 1991, Interferometric Synthetic Aperture Radar interferometry (InSAR) has become a widely used technique for mapping the deformation of the earth's surface caused by earthquakes [e.g., *Massonnet and Feigl*, 1998]. We processed a pair of descending-track ASAR images spanning the earthquake with a time separation of 35 days – the shortest possible repeat time for Envisat – and improved the effective baseline of the resultant interferogram by differencing with a second interferogram constructed from a preseismic pair of ASAR images[1] [*Massonnet and Feigl*, 1998] (Table 1). The topographic contribution to the phase in each interferogram was removed using a digital elevation model (DEM) constructed from an ERS tandem pair (Table 1).

[6] The interferogram (Figure 3a) shows an asymmetric, four-lobed pattern, centred on a north-south oriented discontinuity that is coincident with an incoherent band in the interferogram. The eastern lobes are larger in magnitude than those in the west, with the south-east quadrant moving towards the satellite by ~30 cm, and the north-east quadrant

moving away from the satellite by ~16 cm. West of the discontinuity, the phase changes are smaller, with a range decrease of ~5 cm in the NW and range increase of ~5 cm in the SW. These range changes represent, we believe, the coseismic displacement due to the earthquake – although we cannot rule out the possibility of rapid postseimic deformation, we expect such an effect to be small; an interferogram spanning the interval between 12 and 47 days after the earthquake shows less than 2 cm of range change in the vicinity of Bam (unpublished data, 2004).

[7] To further investigate the discontinuity evident in the interferogram, we calculated the interferometric correlation, a measure of the spatial similarity of radar returns (amplitude and phase) in the interferogram. If the distribution of radar-reflective objects inside a SAR resolution cell changes between the two image acquisitions, the correlation will be reduced. Despite the long spatial baselines, the correlation in the interferograms is generally high, probably due to the low relief, arid environment and short temporal separation. However, the correlation image (Figure 3c) shows that the city of Bam and town of Baravat have a very low degree of correlation. Part of this decorrelation is caused by vegeta-

Table 1. Interferograms Constructed for This Study

	Sensor 1	Date 1	Sensor 2	Date 2	$B_\perp$[a]
preseismic	ASAR	11-Jun-03	ASAR	03-Dec-03	480[b]
coseismic	ASAR	03-Dec-03	ASAR	07-Jan-04	540[b]
DEM	ERS-1	02-Apr-96	ERS-2	03-Apr-96	−129

[a]Perpendicular baseline (metres).
[b]In this study, these interferograms were differenced to form a composite image with an effective baseline of 60 m.

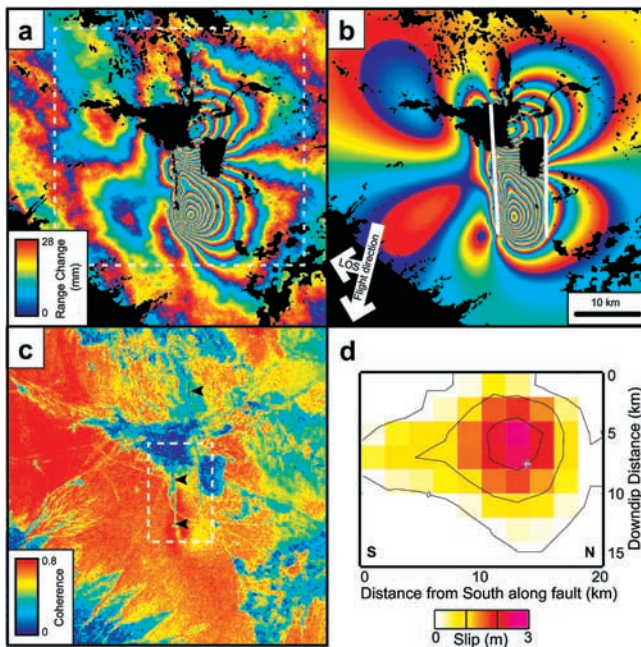[1]Auxiliary material is available at ftp://ftp.agu.org/apend/gl/2004GL020058.

Figure 3. (a) Detail of Envisat ASAR interferogram. [White dotted box: area shown in Figure 1.] (b) Synthetic interferogram of the same area based upon our best-fitting two-fault distributed-slip model. [White lines: surface projections of model fault planes; white arrows: direction of motion of the satellite and pointing direction of the radar antenna.] (c) Interferometric correlation (coherence). [Red colours: high correlation; blue colours: low; black arrows: location of band of low coherence due to surface faulting; white dotted box: location of the enlargements in Figure 4.] (d) The distribution of slip on the main right-lateral strike-slip fault.

tion – Bam and Baravat are important regional producers of dates and citrus fruits. The remainder is due to the high degree of damage sustained in Bam during the earthquake, with more than 50% of the buildings in the city destroyed or badly damaged.

[8] The correlation image also reveals several narrow, linear bands of very low correlation, both north and south of Bam (Figures 3c and 4a); similar features have been shown to represent fault surface ruptures in previous earthquakes [e.g., *Simons et al.*, 2002]. In the north, there is an area of decorrelation coincident with the minor surface ruptures described earlier (Figure 2a). The decorrelation feature south of Bam was not mapped in our original field survey, but aligns with the largest discontinuity in the interferometric phase. Prompted by this discovery, we carried out further field work in this area. We found a series of discontinuous en echelon surface breaks, each 50–100 m long, trending at N 30°E (Figures 2c and 2d) and aligned along the decorrelated band (Figure 4a). The maximum observed offset was 20 cm in a right-lateral sense, with a slip vector that was typically oriented at N 10°E.

3. Determining Fault Parameters Using InSAR

[9] Preliminary seismic focal mechanisms for the earthquake (Figure 1) suggested that it involved predominantly strike-slip motion on a near-vertical fault. To determine a source mechanism from the interferogram, we modeled the co-seismic displacements with slip on a rectangular dislocation in an elastic half space [*Okada*, 1985]. We used a non-linear inversion algorithm [*Wright et al.*, 1999] to solve for the strike, dip, rake, slip, dimensions, location and depth of the fault. To start with, we inverted for uniform slip on a single fault but found that a near-vertical fault, consistent with the NEIC mechanism based on first motions, and with a surface trace located at the linear zone of decorrelation discussed above, leaves large unmodeled decreases in range south of Bam.

[10] If a second, thrust fault is introduced beneath the previously-mapped Bam fault, 5 km to the east of the main rupture (Figure 1), an improved fit to the interferogram is obtained in the area where the single fault model leaves significant residuals. The introduction of a secondary fault is supported by modeling of teleseismic P- and SH-bodywaves which suggests there was a second event ~10 seconds after the mainshock, with about 20% of the seismic moment of the main strike-slip event and consistent with a north-south thrust dipping west at ~30° (Figures A1–A3). In addition, strong motion records from an accelerometer in Bam suggest a second event, showing a broad displacement pulse at 8–10 seconds after the first arrivals (BHRC, Iran, http://www.bhrc.gov.ir/Bhrc/d-stgrmo/shabakeh/earthquake/bam/bam.htm). In calculating the model interferogram we fix the values of strike, dip and rake for the main, strike-slip event (357°, 88°, −166°) and the secondary, thrust fault (180°, 30°, 90°) to the values obtained by seismology.

[11] To determine a more realistic picture of the slip on the faults at depth, we solved for the best-fitting, smooth distribution of slip on the fault planes (Figures 3b and 3d), having extended them spatially in all directions. A good fit to data is obtained, with far-field residuals at the level of atmospheric noise (Figure A4d). For the strike-slip fault we
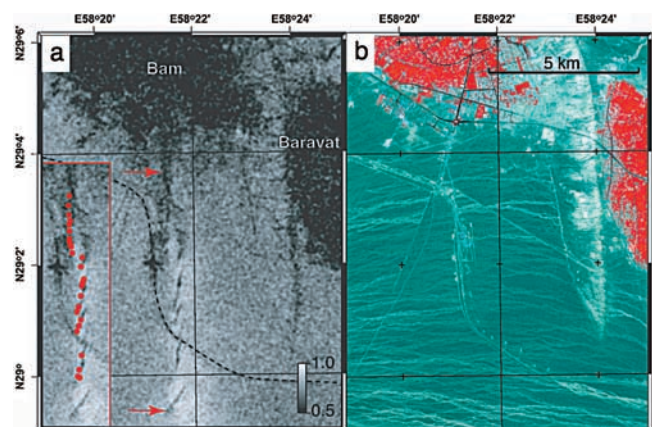

Figure 4. (a) Detail of interferometric correlation south of Bam. The dashed line marks the trace of the railway line that can also be seen in (b). Inset: locations of observed surface breaks plotted over correlation image, showing that they coincide with the black incoherent features. (b) Enlargement of ASTER image for the same area as (a), demonstrating the absence of surface features above the Bam earthquake fault. The previously-identified Bam Fault is easily visible at the right of the image.

find that most slip occurred over a region that is 12 km long and 8 km wide, with a peak slip of 2.5 m at a depth of ~5 km, decaying to a maximum of 0.5 m in the upper 2 km – consistent with our field observations which showed that only a small amount of slip reached the surface (Figures 2c and 2d). Errors in these slip estimates are ≤0.2 m in the upper 10 km of the fault (Figure A5). The secondary, thrust fault slipped up to 1.2 m at depth between the southern end of the main, strike-slip fault, and the previously-mapped Bam Fault. Although non-unique and preliminary, this solution is consistent with both InSAR and seismological observations.

4. Discussion

[12] The main strike-slip fault revealed by InSAR has no surface expression in satellite imagery acquired before the earthquake (Figure 4). Field photographs (Figure 2c) show that the area is a largely featureless plain cut by small drainage channels. It is estimated that the Nayband-Gowk-Sabzevaran fault system only accommodates about 1–2 mm/yr of the 15 mm/yr relative motion between central Iran and Afghanistan [Walker and Jackson, 2002]. As these faults, to the west of Bam, are more pronounced morphologically, it is likely that the strain rate on the fault that failed in the Bam earthquake is only a very small fraction of this total. Given a long likely recurrence interval it is possible that the surficial features of past earthquakes on this fault, likely to be of similar size to those of the 2003 event, will have been obscured by sedimentation – either from infrequent floods or from wind-blown deposits – leaving no trace of the fault at the surface.

[13] Identifying seismogenic faults is a key component of seismic hazard analysis. In the case of buried, or 'blind' faults, it becomes of critical importance. Earthquakes on blind thrust faults are not uncommon, e.g., Tabas, Iran (1978), Northridge, California (1994). Even if there is no historical record of past earthquakes, a blind thrust will produce geomorphological effects that can be recognised, such as drainage incising into topography produced by the thrusting [e.g., Lettis et al., 1997; Walker et al., 2003]. The strike-slip fault at Bam, however, is completely blind – in the absence of an earthquake, no feature in the topography or drainage pattern would have alerted us to its presence. The combination of an absence of any historical reports of past earthquakes at Bam, and the absence of surface features produced by past faulting on the main fault, makes estimating the seismic hazard in such an area extremely difficult.

References

Ambraseys, N., and C. Melville (1982), *A History of Persian Earthquakes*, Cambridge Univ. Press, Cambridge, UK.

Berberian, M., and M. Qorashi (1994), Coseismic fault-related folding during the south Golbaf earthquake of November 20, 1989, in southeast Iran, *Geology*, 22, 531–534.

Berberian, M., and R. Yeats (1999), Patterns of historical earthquake rupture in the Iranian plateau, *Bull. Seismol. Soc. Am.*, 89, 120–139.

Berberian, M., J. Jackson, M. Qorashi, and M. Kadjar (1984), Field and teleseismic observations of the 1981 Golbaf-Sirch earthquakes in SE Iran, *Geophys. J. R. Astron. Soc.*, 77, 809–838.

Berberian, M., C. Baker, E. Fielding, J. Jackson, B. Parsons, K. Priestley, M. Qorashi, M. Talebian, R. Walker, and T. Wright (2001), The 14 March 1998 Fandoqa earthquake (M_w 6.6) in Kerman province, S.E. Iran: Re-rupture of the 1981 Sirch earthquake fault, triggering of slip on adjacent thrusts, and the active tectonics of the Gowk fault zone, *Geophys. J. Int.*, 146, 371–398.

Jackson, J., and D. McKenzie (1988), The relationship between plate motions and seismic moment tensors and the rate of active deformation in the Mediterranean and Middle East, *Geophys. J. R. Astron. Soc.*, 93, 45–73.

Lettis, W., D. Wells, and J. Baldwin (1997), Empirical observations regarding reverse earthquakes, blind thrust faults, and quaternary deformation: Are blind thrusts truly blind?, *Bull. Seismol. Soc. Am.*, 87, 1171–1198.

Massonnet, D., and K. L. Feigl (1998), Radar interferometry and its application to changes in the Earth's surface, *Rev. Geophys.*, 36, 441–500.

Matheson, S. (1976), *Persia: An Archaeological Guide*, 2nd ed., Faber and Faber, New York.

Okada, Y. (1985), Surface deformation due to shear and tensile faults in a half-space, *Bull. Seismol. Soc. Am.*, 75, 1135–1154.

Rosen, P. A., S. Hensley, G. Peltzer, and M. Simons (2004), Updated repeat orbit interferometry package released, *Eos Trans. AGU*, 85, 35.

Simons, M., Y. Fialko, and L. Rivera (2002), Coseismic deformation from the 1999 M_w 7.1 Hector Mine, California earthquake as inferred from InSAR and GPS observations, *Bull. Seismol. Soc. Am.*, 92, 1390–1402.

Walker, R., and J. A. Jackson (2002), Offset and evolution of the Gowk Fault, S.E. Iran: A major intra-continental strike-slip system, *J. Struct. Geol.*, 24, 1677–1698.

Walker, R., J. A. Jackson, and C. Baker (2003), Surface expression of thrust faulting in eastern Iran: Source parameters and surface deformation of the 1978 Tabas and 1968 Ferdows earthquake sequences, *Geophys. J. Int.*, 152, 749–765.

Wright, T. J., B. Parsons, J. Jackson, M. Haynes, E. Fielding, P. England, and P. Clarke (1999), Source parameters of the 1 October 1995 Dinar (Turkey) earthquake from SAR interferometry and seismic bodywave modelling, *Earth Planet. Sci. Lett.*, 172, 23–37.

————————————

E. J. Fielding and P. A. Rosen, Jet Propulsion Laboratory, California Institute of Technology, 4800 Oak Grove Drive, Pasadena, CA 91109, USA.

G. J. Funning, B. Parsons, and T. J. Wright, COMET, Department of Earth Sciences, Parks Road, Oxford OX1 3PR, UK. (gareth.funning@earth.ox.ac.uk)

M. Ghorashi, H. Nazari, and M. Talebian, Geological Survey of Iran, Azadi Square, Meraj Street, PO Box 13185-1494, Tehran, Iran.

J. Jackson, K. Priestley, and R. Walker, COMET, Bullard Laboratories, Madingley Road, Cambridge CB2 0EZ, UK.